Reprint from

PLASMA PHYSICS AND CONTROLLED NUCLEAR FUSION RESEARCH 1994

PROCEEDINGS OF THE
FIFTEENTH INTERNATIONAL CONFERENCE ON PLASMA PHYSICS
AND CONTROLLED NUCLEAR FUSION RESEARCH
HELD BY THE
INTERNATIONAL ATOMIC ENERGY AGENCY
IN SEVILLE, 26 SEPTEMBER–1 OCTOBER 1994

In four volumes

VOLUME 2

INTERNATIONAL ATOMIC ENERGY AGENCY
VIENNA, 1995

VORTICES, HOLES AND TURBULENT RELAXATION IN SHEARED ELECTRON COLUMNS

C.F. DRISCOLL, K.S. FINE, X.-P. HUANG,
T.B. MITCHELL[1], A.C. CASS, T.M. O'NEIL
Department of Physics
and Institute for Pure and Applied Physical Sciences,
University of California at San Diego,
La Jolla, California,
United States of America

Abstract

VORTICES, HOLES AND TURBULENT RELAXATION IN SHEARED ELECTRON COLUMNS.

Magnetically confined electron columns evolve as ideal 2D fluids, allowing quantitative study of shear flow instabilities, vortex formation, turbulence, and self-organization. It is found that rapid global symmetrization of a distorted column can occur by a decay instability due to non-linear beat wave damping. In the free relaxation of turbulence, it is found that the relaxation rate is limited by vorticity holes which persist for hundreds of rotations even in strong background shear. Finally, turbulence is observed to self-organize to a meta-equilibrium state which is accurately predicted by minimization of enstrophy for a range of unstable initial conditions.

1. Introduction

Magnetically confined pure electron columns are excellent systems for observing 2D vortices, turbulence, and self-organization in the presence of background shear flow [1]. The electron columns are confined radially by a uniform magnetic field, B_z, and contained axially by voltages applied to end sections of the cylindrical wall. The confined plasma is sensed and manipulated by antennas in the wall, and the z-averaged electron density $n(r,\theta,t)$ is accurately measured by dumping the column onto a phosphor screen imaged by a 512 × 512 × 16 bit CCD camera.

The axial bounce frequency of an electron is large compared to the $\mathbf{E}\times\mathbf{B}$ drift rotation frequency ($\omega_B \gg \omega_R$), so the flow can be described by the 2D drift-Poisson equations. These are isomorphic to the 2D Euler equations for an incompressible inviscid fluid, and are close cousins to the Hasegawa-Mima equations for drift-wave turbulence. The measured electron density $n(r,\theta,t)$ is proportional to the vorticity of the flow.

We study instabilities and relaxation by creating well-controlled but unstable initial conditions and then observing the free evolution. Shear-flow instabilities

[1] Current address: Los Alamos National Laboratory, High Energy Physics, Los Alamos, New Mexico, United States of America.

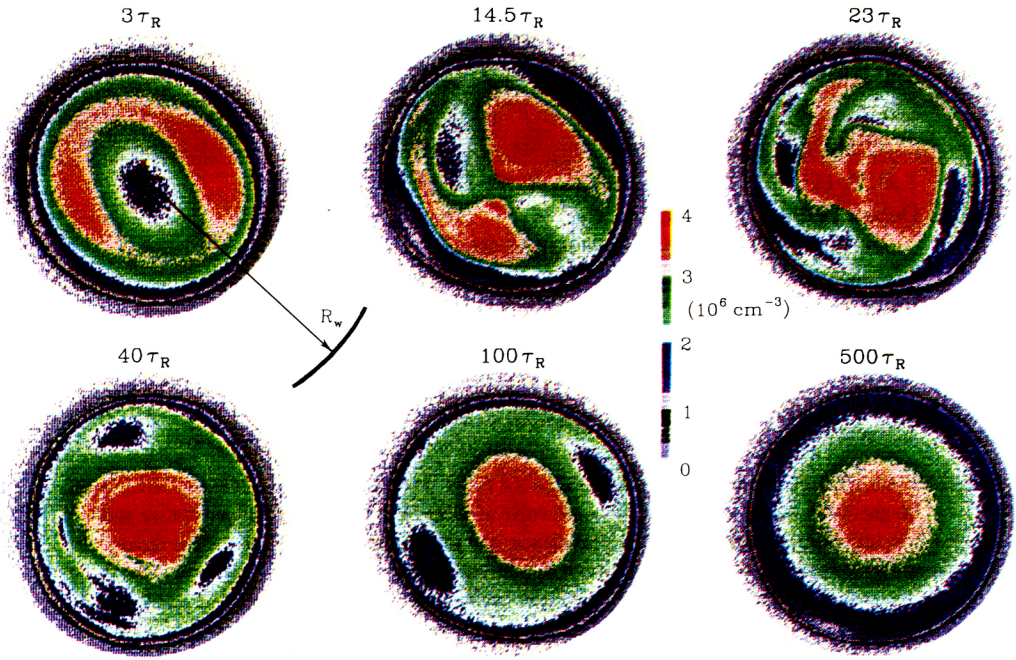

FIG. 1. Contours of the density (vorticity) during instability, vortex driven transport, and relaxation to a meta-equilibrium state.

lead to the formation of vortices, which then merge, shed filaments, and eventually relax to an axisymmetric, sheared meta-equilibrium state (MES). An example of such an evolution is shown in Fig. 1, labeled in bulk rotation times τ_R.

2. Shear Flow Modes and Instabilities

If we start with a smooth, symmetric density profile $n(r)$ and add a small perturbation in θ, we are able to study near-linear modes and instabilities. Our $n(r,\theta,t)$ data allows us to completely characterize the $k_z = 0$ flute modes, varying as $\exp(im\theta - i\omega_m t)$. For hollow profiles, we observe both the expected Kelvin-Helmholtz instabilities and other stable $\mathbf{E}\times\mathbf{B}$ drift, or "diocotron" modes. These modes are not well-predicted by the usual step-profile analysis; however, both the frequencies and growth rates are reasonably well characterized by computational solution of the eigenvalue equation using the measured density profiles [2]. An exception is $m = 1$, where we observe a robust exponential instability [3] where cold fluid theory predicts only algebraic growth; here, FLR and finite length effects may cause the instability [4].

Similar flute modes have been extensively analyzed [5] and have recently been observed in neutral plasmas with electric fields arising from regions of non-neutrality [6,7]. One interesting question is the net charge of the plasma and the effects of image charges in the walls. For cylindrical geometry, the image charges

from a net plasma charge give rise to the stable $m = 1$ diocotron mode, wherein the entire displaced plasma column orbits around the center of the confinement cylinders. For toroidal geometry, this image charge mode would be more complicated.

The stable $m \geq 2$ flute modes can be damped [8] by a spatial resonance at r_s, where $\omega_m = m\,\omega_R(r_s)$, analogous to velocity-space Landau damping. For all readily detectable mode amplitudes, this damping is observed to be nonlinear, in that cat's-eye density filamentation forms around r_s as the mode damps. The observed damping rates are thus substantially less than the predicted linear rates.

Recently we have observed a decay instability [9] in which a nominally undamped mode with amplitude A_m decays to a daughter mode A_{m-1}. This occurs due to spatial Landau damping of the nonlinear beat between the two modes at $\omega_m - \omega_{m-1}$. The daughter mode is observed to grow exponentially, at a rate varying roughly as A_m^2. These rates (normalized by τ_R) are shown in Fig. 2 for mode numbers $4 \rightarrow 3$, $3 \rightarrow 2$ and $2 \rightarrow 1$. Also shown is an initial large amplitude $m = 3$ state and the $m = 2$ state which results 10 τ_R later.

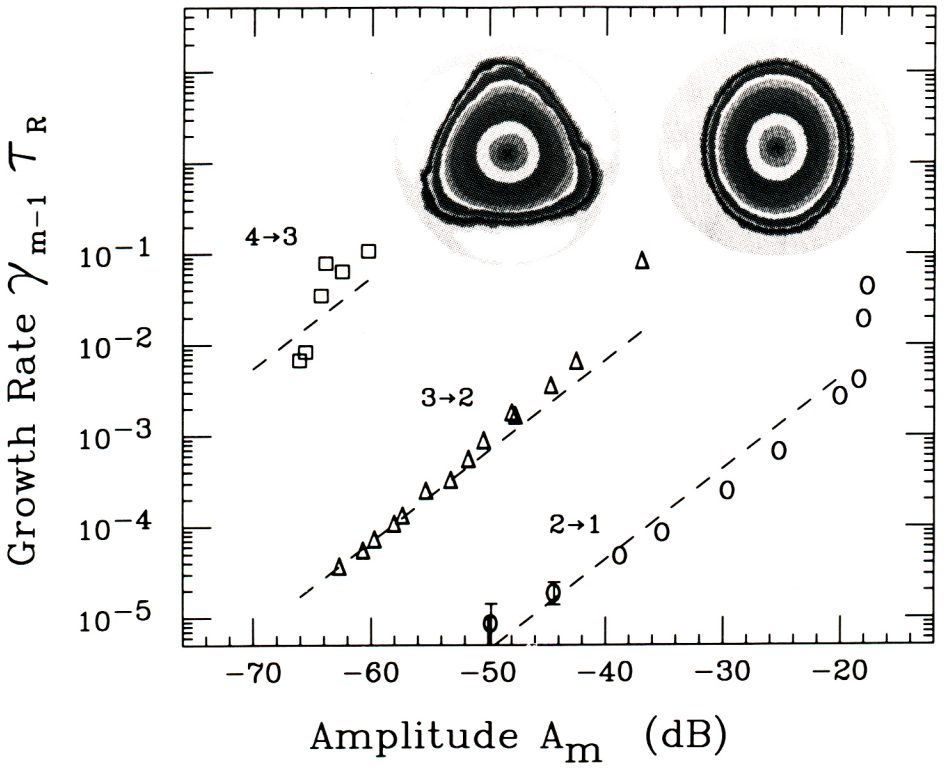

FIG. 2. Measured decay instability growth rates $\gamma_{m-1}\,\tau_R$ versus mode amplitude A_m, for m = 4, 3 and 2. Insert shows $n(r,\theta)$ before and after $3 \rightarrow 2$ instability.

This decay process is seen to give rapid global symmetrization of a distorted column, while presumably also generating fine-scale resonance filaments within the vortex. For highly distorted vortex profiles, this beat wave damping is observed to be an important mechanism for symmetrization.

3. Relaxation of Fluctuations in Shear

Vortices generated by the shear-flow instabilities result in rapid cross-field particle transport to a state which is no longer globally unstable, as at 23 τ_R in Fig. 1. This state can be treated as a sheared θ-averaged background profile, plus turbulent fluctuations on various spatial scales.

We find that the fluctuations then decay about 50 times slower than predicted by simple "passive tracer mixing" in the presence of shear, and that the measured "noise" is strongly skewed from Gaussian [10]. These effects are due to the longevity of "holes," *i.e.* self-trapped regions of negative relative electron density or vorticity. These holes are clearly visible in the fourth and fifth frames of Fig. 1. Figure 3 shows that the shot-to-shot density fluctuations, $\tilde{n}$ (at $r \equiv R/R_w = 0.33$), decay in hundreds of τ_R, whereas a passive tracer would be smeared out in a few τ_R. The probability distribution ρ for measuring density n is strongly skewed towards low densities.

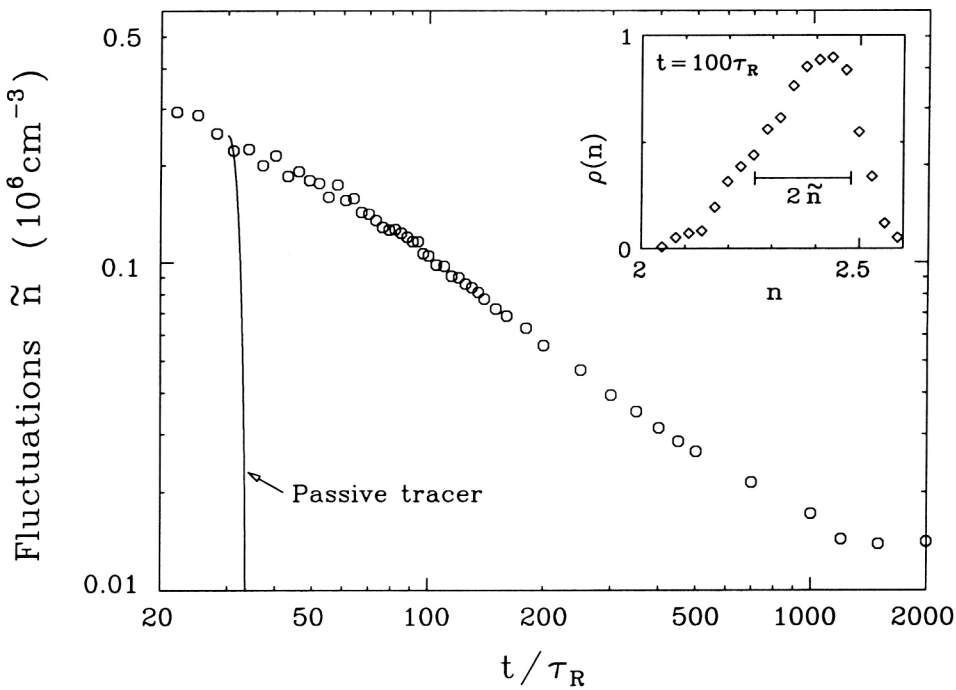

FIG. 3. Measured decay of fluctuations compared to passive tracer prediction, and measured non-Gaussian fluctuation distribution.

A simple fluid model [11] shows that elliptical vortices can be in equilibrium with a weak imposed shear, but are elongated and destroyed by strong shear. Specifically, if the shear is prograde (in the vortex rotation direction), elliptical equilibria exist for all shear strengths; however, strong shear gives unphysically large elongations. If the shear is retrograde, equilibria exist only for weak shear.

Thus, in flows with strong negative shear (i.e. $\partial\omega_R/\partial r < 0$), such as Fig. 1 after $\approx 30\,\tau_R$, density clumps and shallow holes are sheared apart by the background flow, while relatively intense holes remain self-trapped. Measurements of the aspect ratios of these elliptical holes agree with the equilibria predicted for the measured shear [10]. However, we also observe that the holes slowly drift outward (due to unknown effects) and are eventually destroyed. For other evolutions with less shear, intense clumps (i.e. regions of 4× enhanced electron density) are observed to dominate the "noise" at large times.

4. Meta-Equilibrium States

Eventually, the system relaxes to a low-noise meta-equilibrium state (MES). We observe that the MES is axisymmetric with a monotonically decreasing density profile and lasts for about $10^4\,\tau_R$ before non-ideal effects cause it to evolve further [12]. The total number of electrons, angular momentum and electrostatic energy, given by

$$N \equiv R_w^2 \int d^2\mathbf{r}\; n$$

$$P_\theta \equiv \int d^2\mathbf{r}\; (1-r^2)\, n/n_0$$

$$H_\phi \equiv -\frac{1}{2}\int d^2\mathbf{r}\; (n/n_0)\; (\phi/\phi_0)$$

are well conserved from the initial conditions to the MES. Here, $n_0 \equiv N/R_w^2$, and $\phi_0 \equiv eN$. However, less robust "ideal" invariants such as enstrophy and mean-field entropy, given by

$$Z_2 \equiv 1/2 \int d^2\mathbf{r}\; (n/n_0)^2$$

$$S \equiv -\int d^2\mathbf{r}\; (n/n_0)\, \ln (n/n_0)$$

vary significantly, due to measurement coarse-graining or dissipation of small spatial scales.

We have compared the measured MES density profiles to various theories based on maximization of entropy or minimization of enstrophy [13]. We find that minimization of enstrophy accurately predicts the meta-equilibrium profiles for hollow initial conditions of moderate energy [12] such as shown in Fig. 1. These profiles are significantly different from the predictions of maximum entropy. The minimization is subject to constant N, P_θ, and H_ϕ, and to the physical constraint that $n \geq 0$. The explicit P_θ dependence of the solution is removed by rescaling the enstrophy as $\hat{Z}_2 \equiv 4\pi(1-P_\theta)\, Z_2$, and considering the excess energy

$$H_\phi^{\text{exc}} \equiv H_\phi - H_\phi^{\min}$$

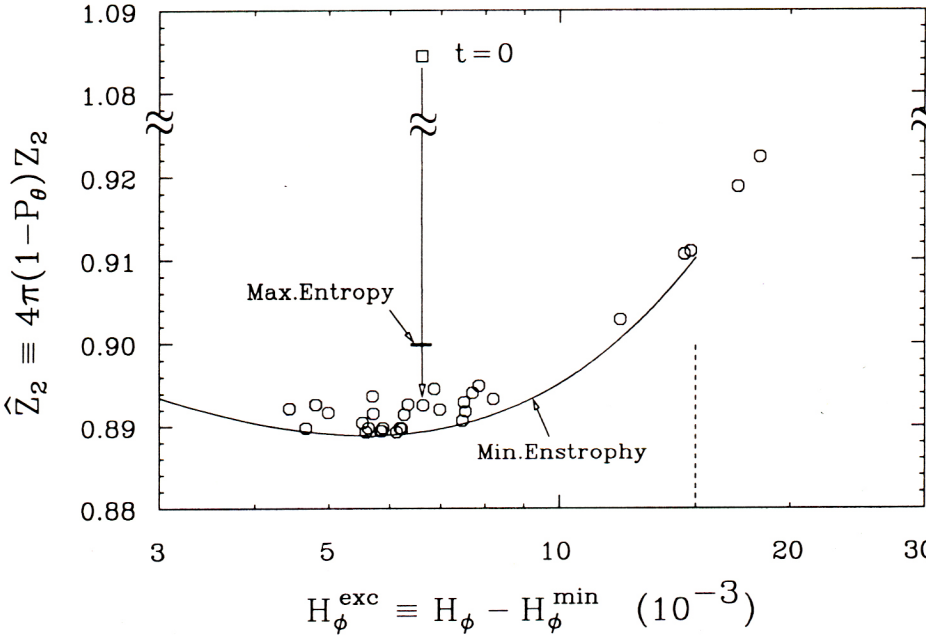

FIG. 4. Predicted (curve) and measured (points) enstrophy $\hat{Z}_2$ versus excess energy H_ϕ^{exc}.

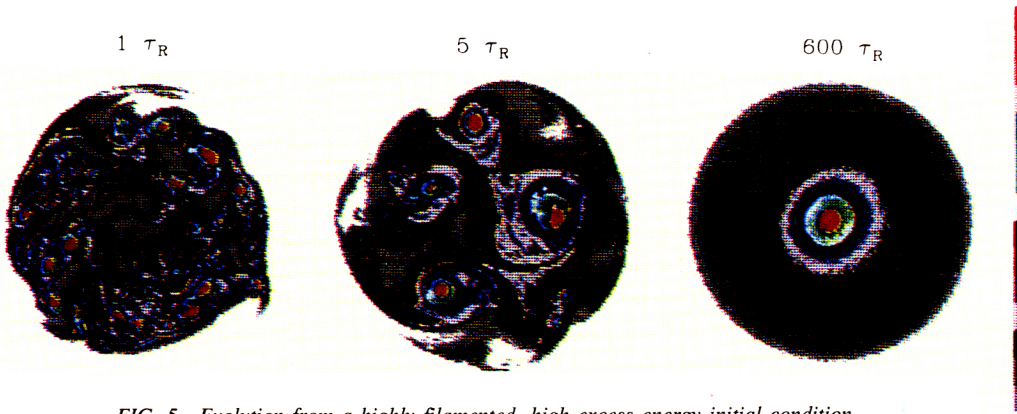

FIG. 5. Evolution from a highly filamented, high excess energy initial condition.

Here, $H_\phi^{\min} \equiv 1/2\,\{1/2 - \ln[2(1-P_\theta)]\}$ is the minimum energy possible for given N and P_θ, i.e. the energy of a uniform density column. Figure 4 shows the measured MES $\hat{Z}_2$ (circles) and the predicted minimum $\hat{Z}_2$ (curve) for a range of excess energies.

We have recently upgraded a containment apparatus to operate at 20 kG, to obtain better spatial and temporal resolution. We are now able to create initial conditions which result in greater fine-scale filamentation than those of Fig. 1, resulting in substantially greater excess energies. Figure 5 shows an evolution with $H_\phi^{\text{exc}} \simeq 45. \times 10^{-3}$. For these cases, substantially different final profiles are observed, and the minimum enstrophy and maximum entropy states can not yet be predicted. However, it is clear that the turbulence self-organizes to a specific state independent of the details of the initial conditions.

Acknowledgments

This work was supported by USDOE Grant DE-FG03-85ER53199, ONR Grant N00014-82-K-0621, and NSF Grant PHY91-20240.

REFERENCES

[1] DRISCOLL, C.F., FINE, K.S., Experiments on vortex dynamics in pure electron plasmas, Phys. Fluids B **2** (1990) 1359.

[2] DRISCOLL, C.F., MALMBERG, J.H., FINE, K.S., SMITH, R.A., HUANG, X.-P., GOULD, R.W., Growth and decay of turbulent vortex structures in pure electron plasmas, Plasma Physics and Controlled Nuclear Fusion Research 1988, **3**, IAEA, Vienna (1989) 507.

[3] DRISCOLL, C.F., Observation of an unstable $l = 1$ diocotron mode on a hollow electron column, Phys. Rev. Lett. **64** (1990) 645.

[4] SMITH, R.A., ROSENBLUTH, M.N., Algebraic instability of hollow electron columns and cylindrical vortices, Phys. Rev. Lett. **64** (1990) 649; SMITH, R.A., Effects of electrostatic confinement fields and finite gyroradius on instability of hollow electron columns, Phys. Fluids B **4** (1992) 287.

[5] HORTON, W., LIU, J., MEISS, J.D., SEDLAK, J.E., Solitary vortices in a rotating plasma, Phys. Fluids **29** (1986) 1004.

[6] HULD, T., NIELSEN, A.H., PECSELI, H.L., RASMUSSEN, J.J., Coherent structures in 2D plasma turbulence, Phys. Fluids B **3** (1991) 1609.

[7] SONG, B.,. SEN, A.K., Flow-shear stabilization of ion-temperature-gradient-driven instability in a linear machine, Phys. Rev. Lett. **72** (1994) 92.

[8] BRIGGS, R.J., DOUGHERTY, J.D., LEVY, R.H., Role of Landau damping in crossed-field beams, Phys. Fluids **13** (1970) 421.

[9] MITCHELL, T.B., DRISCOLL, C.F., Symmetrization of 2D vortices by beat-wave damping, Phys. Rev. Lett. (1994).

[10] HUANG, X.-P., Experimental Studies of Relaxation of 2D Turbulence in Magnetized Electron Plasma Columns, PhD Thesis, U. Calif. San Diego (1993).

[11] MOORE, D.W., SAFFMAN, P.G., Aircraft Wake Turbulence and its Detection, Plenum, New York (1971) 339.

[12] HUANG, X.-P., Driscoll, C.F., Relaxation of 2D turbulence to a meta-equilibrium near the minimum enstrophy state, Phys. Rev. Lett. **72** (1994) 2187.

[13] KRAICHNAN, R.H., MONTGOMERY, D., Two-dimensional turbulence, Rep. Prog. Phys. **43** (1980) 547.